Transactions of the Materials Research Society of Japan 33[2] 323-326 (2008)

Counterion Immobilization in a Strong Polyelectrolyte Brush by Zeta Potential Measurements

Takuya Fujima, Takashi Okano, Nagahiro Saito* and Osamu Takai
EcoTopia Science Institute, Nagoya University, Furo-cho, Chikusa, Nagoya 464-8603, Japan
*Graduate School of Engineering, Nagoya University, Furo-cho, Chikusa, Nagoya 464-8603, Japan
e-mail: fujima_t@eco-t.esi.nagoya-u.ac.jp

The counterion immobilization has been investigated about a brush configuration of a strong polyelectrolyte, sodium polystyrene sulfonate (NaPSS). Zeta potential of the planar NaPSS brushes was measured under a variety of salt, sodium chloride (NaCl), concentration conditions. Analysis based on Poisson-Boltzmann equation provided the amount of counterion that was unimmobilized and hydrodynamically mobile outside the brush layer. Its salt concentration dependence revealed the counterion immobilization to be weakened by the salt addition with following a power law between the unimmobilized counterion rate and the added salt concentration.

1. INTRODUCTION

Charged polymers densely grafted onto surface of solid substrates or colloids configure polyelectrolyte brushes [1–3]. The system is attracting a lot of interest from both scientific and engineering viewpoints: balance between molecular confinement of the polymer chains onto the substrate and coulombic interactions among ions, and its potential for application as new "smart surfaces" which realizes surface property switching, nano-particle actuation and so on [3]. Another remarkable topic is its high biocompatibility. Protein immobilization on the charged brush surface with keeping the protein structures nearly unchanged is a hot topic in recent years [4].

Polymer brush systems has been researched since clues theoretically given about neutral [5-6] and charged [7-8] system. Though they have stimulated a lot of studies in mainly theory and simulation, experimental ones are scarce because of substantial difficulties in sample preparation. Many of the experimental researches are about swelling of weak polyelectrolyte brushes. Segment density profile in the brush layers has been investigated under various conditions by using neutron, X-ray, ellipsometry, AFM and so on [9–14].

Spacial distribution of counterions in the polyelectrolyte brush system is one of the most primitive and important topics not only for the fundamental statistical physics but also for the protein adsorption. However, there are only a few experimental approaches to this topic by neutron reflectivity [15] and small angle X-ray scattering (SAXS) [16–18]. They have provided volume fraction profile of the counterion as a function of distance from the substrate surface. Detailed experimental investigation about the dependency of the counterion behavior on parameters like temperature, pH and salt conditions has not been carried out. That is also true as to how much amount of the counterion is immobilized in the brush layer or freely mobile from the hydrodynamical viewpoint. These topics are thought to be essential to understand the adsorption mechanism of proteins on the polyelectrolyte brushes because the phenomenon strongly depends on ionic conditions: the adsorption and desorption proceed under low and high ionic strength circumstances, respectively.

We thus explored the counterion immobilization in a polyelectrolyte brush by using zeta potential measurements. The experimental principle differentiates hydrodynamically immobilized and fluid layer by detecting the electroosmotic flow induced on the sample. Then the measurements gives electrostatic potential on the slip plane, the border of fluid and non-fluid layers. We adopted a strong polyelectrolyte, sodium polystyrene sulfonate (NaPSS), for the brush configuration to suppress the change of ionic dissociation rate under a variety of ionic condition which should affect zeta potential [19]. We then performed zeta potential measurements with varying the added salt, sodium chloride (NaCl), concentration and analyzed the result by Poisson-Boltzmann equation. This provided the amount of counterion that was unimmobilized from the polyelectrolyte brush layer and its detailed dependency on the salt concentration as reported below.

2. SAMPLE

The polyelectrolyte brushes were prepared by "grafting-to" method: we first synthesized trichlorosilane-ended polystyrene (PS-$SiCl_3$) by anion polymerization, grafted them onto silicon wafer then sulfonated them to obtain NaPSS brush. The preparation and characterization were carried out by following Tran and Auroy's method [20]. All the chemicals used below were with the highest purity available from Wako Pure Chemical Industries and Kanto Chemical.

Polystyrene (PS) was synthesized by anionic polymerization for monodispersity of molecular weight. We distilled styrene monomer twice to remove contained polymerization retarder and other impurity. Benzene was also distilled directly into the reaction flask where the purified styrene had already been in. All the distillation process above were carried out over lithium-aluminium hydride (LiAlH) with a distillation line filled with

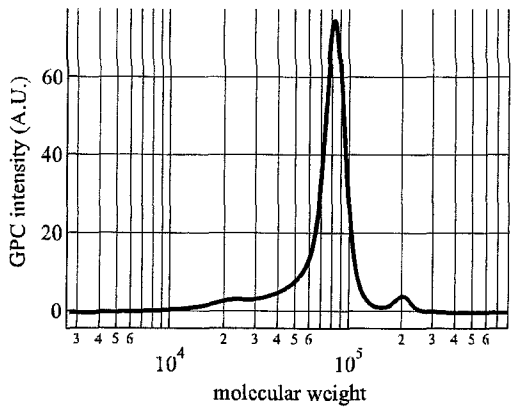

FIG. 1: GPC chart for the polystyrene synthesized by anionic polymerization. Only the main product is to be grafted on substrate to form brush structure.

carefully dried nitrogen gas to eliminate H_2O. The polymerization proceeded at 60 °C for 3 hours after initiated by sec-butyllithium. A small part of the synthesized polystyrene was terminated with methanol to obtain nonreactive polystyrene (PS-H) for molecular weight analysis, and the other part with tetrachlorosilane ($SiCl_4$) for the grafting process. Benzene and excess $SiCl_4$ were removed from the reactive polystyrene (PS-$SiCl_3$) solution by lyophilization and new solvent, toluene, was then added.

We performed gel permeation chromatography (GPC) on the PS-H sample using three analytical columns, TOSOH G4000HHR, arrayed in series with tetrahydrofuran as the eluent. The obtained GPC chart (Fig. 1) showed three peaks with a number average molecular weight of 66 kg/mol and its dispersion (M_w/M_n) of 1.22 in the aggregate. The main component and the two subcomponents had their peaks at molecular weight of 84, 203 and 24 kg/mol, respectively in linear polystyrene equivalent. The main peak was attributed to the linear polystyrene of which the anionic reaction site had been alive till the end of reaction and just capped by methanol, and a long tail on the lower molecular weight side to polymer chains with various polymerization index devitalized during the polymerization process by H_2O leaked into the reactor. The tiny subcomponent on the tail was also from the halfway-devitalized chains but showed a peak since the polymerization initiator was injected into the reaction flask in twice with few-second time lag, and would have been buried in the tail if the injection had carried out at one time. The other subcomponent with larger molecular weight was from a trimer of the main product initiated by CO_2 during the methanol termination process. Therefore, only the main part of the main component without the tail part was to have the ability to be grafted onto the substrates after the $SiCl_3$-termination, of which M_w/M_n was determined to be 1.07.

The PS-$SiCl_3$ was then densely grafted onto (111) surface of n-type silicon wafer by covalent bonding. Silicon wafers, with a typical size of 15 x 35 mm and thickness of 0.52 mm, were first washed in acetone, ethanol and water by ultrasonication then dried by an air jet and a vacuum drier. The wafers were immersed into the toluene solution of PS-$SiCl_3$ under atmosphere typically of 25 °C and 50 % relative humidity immediately after its surface modification into silanol, Si–OH, by an exposure to vacuum UV/ozone for 30 minutes. After the immersion for an hour, the wafers were immediately vacuum dried then heated in dried nitrogen at 160 °C for typically 15 hours to complete the covalent bonding. The obtained PS brushes were rinsed in toluene and vacuum dried.

Ellipsometry on the PS brushes determined graft density of the chains. The grafting density, D, was described as $D = h\,d\,N_A\,M_w^{-1}$. Here, h was dry thickness of the PS layer given by ellipsometry. M_w and N_A were the molecular weight and the Avogadro's number. Weight density of dried PS, d = 1.06 g/cm^3 , was used. The graft density varied around 5 chains for each 100 nm^2 with the grafting condition though the density was homogeneous within a single chip. This proved high grafting density considering the chain length.

Sulfonation of the PS brushes took place in a mixed solution of 16.6 ml of 1,2-dichloroethane, 3.4 ml of acetic anhydride and 1.2 ml of sulfuric acid at 65 °C for typically 3 hours. The sulfonated brushes, polystyrene sulfonic acid brush (HPSS brush), were rinsed in ethanol then immediately immersed into 0.5 mol/dm^3 $NaHCO_3$ aqueous solution to exchange the counterions and obtain NaPSS brush for chemical stabilization.

Infrared absorption spectra was measured before and after the sulfonation to evaluate the sulfonation degree and degrafting rate of the brush chains during the sulfonation process. 2924 cm^{-1} and 3026 cm^{-1} bands corresponded to asymmetric CH_2 stretching and monosubstituted phenyl C-H stretching, respectively. Because the former intensity was proportional to the amount of alkyl segment and the latter to unsulfonated styrene unit, the comparison of the spectra between before and after the sulfonation provided the evaluation. The small amount of polymer in the single layer on the substrate, however, caused low spectral signal-to-noise ratio despite the high sensitivity of the FT-IR spectrometer, DIGILAB FTS7000. The degrafting rate turned out to be less than a tenth, and sulfonation to proceed for all monomer units within the brushes since the 3026 cm^{-1} band disappeared after the sulfonation. The influence of this uncertainty in the sulfonation and degrafting rate will be mentioned in discussion section.

3. ZETA POTENTIAL MEASUREMENTS

The zeta potential measurement system we used in this work, Photal ELS-7300K, was applicable to planar sample by using a quartz cell with a 1-mm thick rectangular parallelepiped water passage open to the sample surface in a rectangular shape of 5 mm x 26 mm. The passage, of which one wall was the sample surface, was filled with water containing added salt and monodisperse latex particle with a diameter of 520 nm as the monitor particle for dynamic light scattering (DLS) measurements. Measuring electroosmotic flow profile in the passage by DLS technique provided electrostatic potential at the hydrodynamic slip plane on the sample, that is, zeta potential. Monodispersity of the polyelectrolyte molecular weight should maintain smooth electroosmotic flow by flat brush surface. The added salt concentration in the filled water, C_s , were controlled in a

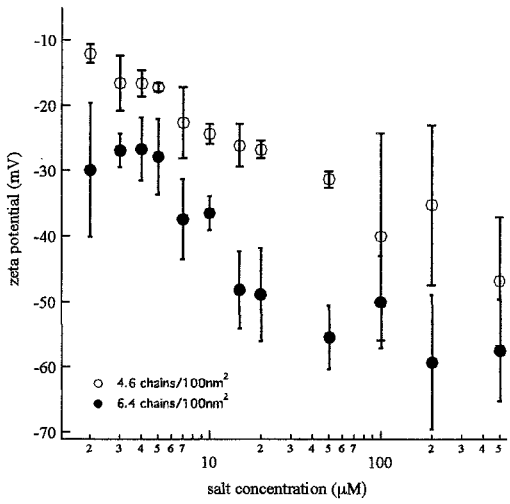

FIG. 2: Salt concentration dependence of zeta potential for NaPSS brushes with different polymer graft density. Open and filled circles are for 4.6 and 6.4 chains/100 nm^2, respectively.

range from 2.0 μM up to 0.50 mM for detailed dependency. Salt free condition was unavailable as the purchased undiluted dispersion liquid of the monitor particle contained 10 mM of NaCl from the first for the micelle stabilization. All the measurements were performed at 25.0 ± 0.1 °C.

Measurement accuracy and reproducibility was carefully checked in several ways. Prior to every set of measurement, we performed reference measurements on materials whose zeta potential was well established like glass slide and bare silicon substrate [21] to check the whole measurement system. A series of measurements about various salt concentration was carried out with increasing then decreasing C_s, which verified the stability of sample during the series of measurements. Reproducibility was also checked by repeatedly performing the same measurements at wide intervals like several weeks. The electroosmotic flow was induced by an appropriate range of electric bias where zeta potential results were independent from the bias intensity, 13-20 V/cm. Each single measurement was carried out with fresh water with added salt and monitor particle to eliminate the electrolytic change of the salt concentration.

Figure 2 shows the added salt concentration dependence of obtained zeta potential for the NaPSS brushes with graft density of 4.6 and 6.4 chains/100 nm^2 in a single logarithmic plot. The zeta potential gains its absolute value along with C_s increase.

4. ANALYSIS and DISCUSSION

Then the zeta potential was analyzed by Poisson-Boltzmann equation (eqs. 1) to extract the information about the counterion immobilization.

$$\begin{aligned} \Delta\Psi(r) &= -\frac{e}{\epsilon}(-\rho_{\mathrm{poly}}(r)+\rho_{\mathrm{Na}}(r)-\rho_{\mathrm{Cl}}(r)) \\ \rho_{\mathrm{Na}}(r) &= \rho_{\mathrm{Na}\cdot 0}\exp(-\frac{e\Psi(r)}{kT}) \\ \rho_{\mathrm{Cl}}(r) &= \rho_{\mathrm{Cl}\cdot 0}\exp(\frac{e\Psi(r)}{kT}) \end{aligned} \qquad (1)$$

where Ψ and ρ are electrostatic potential and number density of each charge as functions of the spatial position r. ϵ, e, k and T for dielectric constant of water, elementary charge, Boltzmann constant and temperature, respectively. Density functions for small ions, ρ_{Na} and ρ_{Cl}, follow the Boltzmann distribution though that for the polyions, ρ_{poly}, does not because of their chemical confinement on the polymer chains. What to be noted here is that ρ_{Na} corresponds to total density function for the counterion from NaPSS brush and added salt cation since they can not be differentiated from each other.

Equations 1 is evolved for planar polyelectrolyte brush system by reducing its dimension to one that is parallel to the normal vector of the sample. The coordinate, r, is set to be zero on the slip plane directing away from the brush, which keeps the position of $r = 0$ outside the brush layer no matter how the brush swelling condition changes. Equation 2 is then derived from eqs. 1 about planar polyelectrolyte brushes in water with added salt[22, 23].

$$\sigma = -2\sqrt{2kT\epsilon C_s}\sinh[\frac{e\Psi(0)}{2kT}] \qquad (2)$$

where $\Psi(0)$ corresponts the zeta potential as is the electrostatic potential on the slip plane. σ is the amount of counterion freed from the polyelectrolyte brush over each unit area of sample surface.

Equation 2 converts the zeta potential data shown in Fig. 2 to the rate of the counterion that is not immobilized in the brush layer but hydrodynamically mobile in water. Figure 3 shows C_s dependence of the rate in a double logarithmic plot. The uncertainty about degrafting rate in the sulfonation process which has been determined by FT-IR affects only with in the range of measurement deviation shown as the errorbars. As shown in the figure, the counterion immobilization behavior of the two samples with different graft density of polyelectrolyte chains are identical, which indicates a universality of this dependency. A power law this dependency follows has a index of 0.7.

This power law about counterion immobilization may be impenetrable at the first glance because the

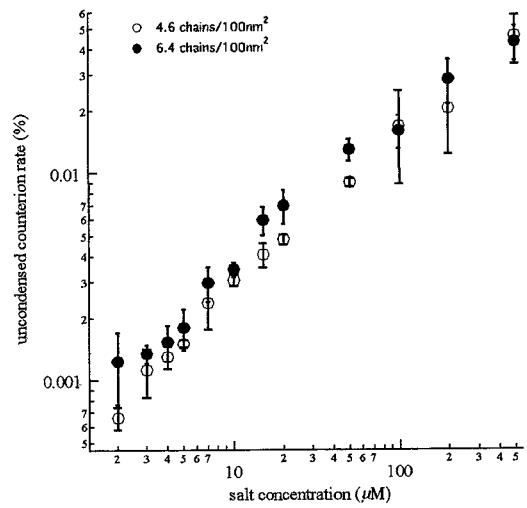

FIG. 3: Added salt concentration dependence of the unimmobilized counterion rate: a power law with its index of 0.7. Markers correspond to the same as in Fig. 2.

counterion "condensation" is predicted to be weakly dependent on added salt concentration by Oosawa-Manning condensation theory. Here, the immobilization in this work has to be differentiated from counterion "condensation". The latter deals with the counterion condensed closely onto polyelectrolyte chains. The former is based on hydrodynamical differentiation of counterion in the larger scale structure of the brush. That is, there are three categories of counterion: (a) condensed onto polyelectrolyte chains, (b) not condensed on the chains but trapped and immobilized in brush layer and (c) hydrodynamically mobile with water outside the slip plane. This categorization is similar to the three-state models proposed about polyelecrtolyte solution [26] and polyelectrolyte star [27].

In comparison with the Bjerrum length (0.71 nm) and Debye screening length (1.1-1.3 nm for our sample) [24], average distance among the grafted chains is obviously large: 7.1 and 6.0 nm. Therefore, most of the space inside the brush layer is for "uncondensed" counterion which is about a third of all counterion in NaPSS case according to the Oosawa-Mannning theory. The densely grafted polyelectrolyte brush strongly attract and immobilize the uncondensed counterion into this space in low C_s condition. The added salt ions are expected to go inside the brush layer because the layer is almost neutralized by immobilizing most of its own counterions in its interior. Ionic concentration in the brush layer increases under high C_s condition to cause stronger electrostatic screening therein. Then counterion is expected to be less attracted from the brush and unimmobilized.

5. CONCLUSION

Counterion immobilization in a strong polyelectrolyte brush has been investigated by performing zeta potential measurements. We achieved quantification of the immobilization by utilizing the principle of the measurement that differentiated ions immobilized and hydrodynamically mobile outside the brush. The added salt concentration dependence of the counterion immobilization has revealed the immobilization attenuated by increase of added salt concentration with following a power law. Then this unimmobilization has been speculated to be attributable to the distribution change of couterions that is not condensed but trapped inside the brush layer.

ACKNOWLEDGEMENT

We thank Prof. Takano and Mr. Yamada for GPC analysis and discussion, also Prof. Seki and Prof. Frusawa for valuable discussions. This research was financially supported by Science Promotion Program of Nagoya University and Foundation Advanced Technology Institute (ATI).

References

[1] J. Rühe, M. Ballauff, M. Biesalski, P. Dziezok, F. Gr. ohn, D. Johannsmann, N. Houbenov, N. Hugenberg, R. Konradi, S. Minko, M. Motornov, R. R. Netz, M. Schmidt, C. Seidel, M. Stamm, T. Stephan, D. Usov and H. Zhang, Adv. Polym. Sci. 165, 79 (2004).

[2] P. M. Claesson, E. Poptoshev, E. Blomberg and A. Dedinaite, Adv. Colloid Interface Sci. 114-115, 173 (2005).

[3] M. Ballauff and O. Borisov, Current Opinion Colloid Interface Sci. 11, 316 (2006).

[4] A. Wittemann and M. Ballauff, Phys. Chem. Chem. Phys. 8, 5269 (2006).

[5] J. Alexander, J. Phys. 28, 977 (1977).

[6] P. G. de Gennes, Macromolecules 13, 1069 (1980).

[7] P. Pincus, Macromolecules 24, 2912 (1991).

[8] O. V. Borisov, T. M. Birshtein and E. B. Zhulina, J. Phys II 1, 521 (1991).

[9] Y. Mir, P. Auroy and L. Auvray, Phys. Rev. Lett. 75, 2863 (1995).

[10] P. Guenoun, F. Muller, M. Delsanti, L. Auvray, Y. J. Chen, J. W. Mays and M. Tirrell, Phys. Rev. Lett. 81, 3872 (1998).

[11] H. Ahrens, S. Förster, C. A. Helm, N. A. Kumar, A. Naji, R. R. Netz and C. Seidel, J. Phys. Chem. B 108, 16870 (2004).

[12] G. R. Lemonne, J. Daillant, P. Guenoun, J. Yang and W. Mays, Phys. Rev. Lett. 93, 148301 (2004).

[13] M. Biesalski, J. Rühe and D. Johannsmann, J. Chem. Phys. 111, 7029 (1999).

[14] M. Gelbert, M. Biesalski, J. Rühe and D. Johannsmann, Langmuir 16, 5774 (2000).

[15] Y. Tran, P. Auroy, L-T. Lee and M. Stamm, Phys. Rev. E 60, 6984 (1999).

[16] F. Muller, P. Fontaine, M. Delsanti, L. Belloni, J. Yang, Y. J. Chen, J. W. Mays, P. Lesieur, M. Tirrell and P. Guenoun, Eur. Phys. J. E 6, 109 (2001).

[17] N. Dingenouts, M. Patel, S. Rosenfeldt, D. Pontoni, T. Narayanan and M. Ballauff, Macromolecules 37, 8152 (2004).

[18] D. Bendejacq, V. Ponsinet and M. Joanicot, Eur. Phys. J. E 13, 3 (2004).

[19] H. Matsumoto, Y. Koyama and A Tanioka, Langmuir 17, 3375 (2001).

[20] Y. Tran and P. Auroy, J. Am. Chem. Soc. 123, 3644 (2001).

[21] H. Sugiyama, A. Hozumi, T. Kameyama and O. Takai, Surf. Interface Anal. 34, 550 (2002).

[22] H. Ohshima and T. Kondo, Biophys. Chem. 39, 191 (1991); H. Ohshima, in *Zeta Potential* edited by A. Kitahara, K. Furusawa, M. Ozaki and H. Ohshima (Scientist Press, Tokyo. 1995).

[23] R.J. Hunter, in *Introduction to Modern Col loid Science* (Oxford University Press, New York. 1993).

[24] M. Gueron and G. Weisbuch, J. Phys. Chem. 83, 1991 (1979).

[25] X. Guo and M. Ballauff, Phys. Rev. E 64, 051406 (2001).

[26] E. Y. Kramarenko, A. R. Khokhlov and K. Yoshikawa, Macromol. Theory Simul. 9, 249 (2000).

[27] A. Jusufi, C. N. Likos and H. Löwen, J. Chem. Phys. 116, 11011 (2002).

(Recieved September 5, 2007 ; Accepted December 10, 2007)